LABORATORY INVESTIGATIONS ON THE THERMOPHYSICAL PROPERTIES OF THE ICE-SNOW INTERFACE WHILE UNDER A CONTROLLED TEMPERATURE GRADIENT

Kevin Hammonds[1]*, Ross Lieb-Lappen[1], Zoe Courville[2], Arnold Song[2], Xuan Wang[1] and Ian Baker[1]

[1]Thayer School of Engineering at Dartmouth College, Hanover, NH, USA
[2]U.S. Army Corps of Engineers, Cold Regions Research and Engineering Laboratory, Hanover, NH, USA

ABSTRACT: Of critical importance to avalanche forecasting is the ability to draw meaningful conclusions from potentially only a small handful of field observations. With this in mind, our research focuses on the development of a new field metric for estimating the likelihood and rate at which new ice crystal growth and kinetic snow metamorphism may be occurring on or near a buried ice lens or crust that is based solely on the thickness of the ice lens and the field-measurable temperature gradient. While both previous literature and theory predict that the presence of an ice lens can act both as a natural barrier to the diffusion of water vapor in the snowpack and as an interface of differential thermal conductivities, no such direct measurements have ever been successfully made in order to characterize or quantify this presumed effect. Presented here, we have developed a laboratory technique that has allowed us to show via in-situ measurements that a super-temperature gradient of several factors greater than the bulk temperature gradient does indeed exist within a millimeter above and below the surface of an artificially created ice lens when placed between two layers of natural snow and held under a controlled temperature gradient. Additionally, we have also investigated the type of new ice crystal growth and kinetic snow metamorphism that has occurred as a result of such a super-temperature gradient existing near the ice lens/snow interface. For this portion of the research, we have utilized Scanning Electron Microscopy for the characterization of ice crystal type and time-lapse X-ray Micro-Computed Tomography to quantify the rates of change in the parameters of interest related to kinetic snow metamorphism, such as the specific surface area and mean grain diameter.

KEYWORDS: kinetic snow metamorphism, crystal growth, temperature gradient, ice lens, μ-CT, SEM

1. INTRODUCTION

It is well known that in perennial mountain snowpacks, it is the natural creation of an ice lens (or crust) on the surface of the snowpack that often leads to dangerous and potentially widespread avalanche conditions later on. This phenomenon can sometimes be directly contributed to accelerated rates of kinetic snow metamorphism and the resultant weakly-bonded and faceted snow grains in the areas adjacent to the newly formed ice lens, creating potentially very weak layers within the snowpack. The longstanding question of exactly what types of ice lenses and under what thermophysical conditions (i.e. temperature gradients and effective thermal conductivities) will lead to the formation of such weak layers and resultant widespread avalanche activity, however, remains largely unanswered. In this study, we have sought to develop a systematic laboratory approach for both better understanding the thermophysical processes associated with the ice/snow interface within a snowpack as well as providing avalanche forecasters with a new metric for better analyzing their field collected data.

In the work presented below, which is still ongoing, we have established a reproducible laboratory method for creating polycrystalline lenses of ice to be placed between two layers of natural snow within an enclosed capsule and observed while under a controlled temperature gradient. Our observations made via time lapse X-ray Micro-Computed Tomography (μ-CT) have thus far been able to capture, to a 15 μm resolution, the kinetic growth of newly formed ice crystals on the bottom of the ice lens as well as the kinetic snow metamorphism of the snow grains immediately adjacent to the ice lens. Post-test analysis of the ice lens via scanning electron microscopy (SEM) has further revealed that while the top (lower temperature) side of the ice lens has remained smooth in texture, the bottom (warmer temperature) side has been altered significantly through water vapor deposition and has grown sharp cornered ice crys-

* *Corresponding author address:*
Kevin Hammonds, Thayer School of Engineering at Dartmouth College, 14 Engineering Drive, Hanover, NH 03755; tel: 970-481-2745; email: kevin.d.hammonds.th@dartmouth.edu

tals with no apparent preference in crystallographic orientation.

We have also had some success in being able to make in-situ temperature measurements of our laboratory prepared specimen, where we have placed several AWG 40 (80 μm) micro-thermocouples within a span of less than 1 mm above and below the ice lens in order to capture the local temperature gradient. We feel these findings have been quite significant, as they have shown that the local temperature gradient near the ice/snow interface can be several times larger than the imposed bulk temperature gradient, in direct support of the long-standing hypothesis that a super-temperature gradient must exist at the ice/snow interface (Greene 2007). Additionally, these results also underline the common field observation that small faceted crystals tend to exist just above or below a buried ice lens in the snowpack (Colbeck and Jamieson 2001).

2. BACKGROUND

Within any given snowpack, it is the thermodynamic processes of both conduction and the release of latent heat that are generally responsible for the overall metamorphic state and resulting microstructure of the snowpack (Armstrong 1985). Mathematically, such a relationship would be best described by the 3-D heat equation, as shown in Eq. (1), where ρ is taken to be the density of snow, c_p is the specific heat capacity of snow at constant pressure, and $\boldsymbol{q}$ the heat flux via conduction or latent heating.

$$\rho c_p \frac{\partial T}{\partial t} = -\nabla \cdot (\boldsymbol{q}_{ice\ conduction} + \boldsymbol{q}_{latent\ heat}) \quad (1)$$

For the instance where the heat exchange in the vertical direction is much greater than in the horizontal direction, such as in this study, Eq. (1) can be reduced to a 1-D representation, as shown in Eq. (2), where k_e is the effective thermal conductivity, a variable that is meant to capture the overall input of thermal conduction through the ice matrix as well as the latent heat transfer of diffusion.

$$\rho c_p \frac{\partial T}{\partial t} = \frac{\partial}{\partial z}\left(k_e \frac{\partial T}{\partial z}\right) \quad (2)$$

In the treatment presented here, we have neglected a convection term based on the work of Gibson and Ashby (1997) and Greene (2007), which show that it is unlikely that the viscous force of water vapor is overcome by the buoyancy force created with the differential heating of a specimen of our spatial dimensions.

While several theoretical studies have been conducted to investigate the effects of these thermodynamic interactions on snowpack metamorphism and stability (Adams and Brown 1990; Colbeck 1991; Colbeck and Jamieson 2001) few have been laboratory tested. One study, however, that did combine field and laboratory testing, upon which the research being presented here is closely related, was that of Greene (2007). Greene conducted a series of laboratory experiments with both naturally occurring and artificially created ice lenses in order to investigate the effects that a temperature gradient may have upon a buried ice layer. Although Greene was ultimately unable to show an increase in the temperature gradient around the ice layer, he did note in his conclusions that some potential reasons for not being able to show this increase in temperature gradient might have been simply due to either insufficient thermocouple sensitivity or too much distance between the thermocouple probes. Additionally, Greene employed a serial sectioning and stereographic 3-D reconstruction technique that is not too dissimilar, phenomenologically speaking, to that of the 3-D reconstruction that takes place as part of a standard μ-CT analysis. During this segment of his research, Greene made several qualitative observations pertaining to the growth of faceted crystals on the bottom of the ice lens, while sublimation and consequent smoothing was taking place on the upper face of the ice lens. Interestingly, around the same time period as Greene, similar field and laboratory observations were made in the Antarctic Megadunes during a field campaign led by the U.S. National Snow and Ice Data Center (Courville 2007), who had also used a dimethyl phthalate pore filler in order to freeze-cast their snow samples for laboratory analysis. However, these were only snapshots of the metamorphic state of the snowpack, as opposed to a temporal evolution, which is what we have aimed to provide here from a strict laboratory standpoint.

3. EXPERIMENTAL METHOD

Our experimental design begins with the creation of a polycrystalline ice specimen that is random in its crystallographic orientation with mean grain size of approximately 1 mm. The intention of these particular specifications is to best represent a naturally-occurring ice lens that is of very low porosity and permeability, such as a rain or possibly

melt-freeze induced ice layer. Using a radial freezing technique developed by Cole (1979), seed grains are flooded under vacuum by chilled liquid water, and we can then verify the random crystallographic orientation of the specimen with polarized light microscopy (Fig. 1).

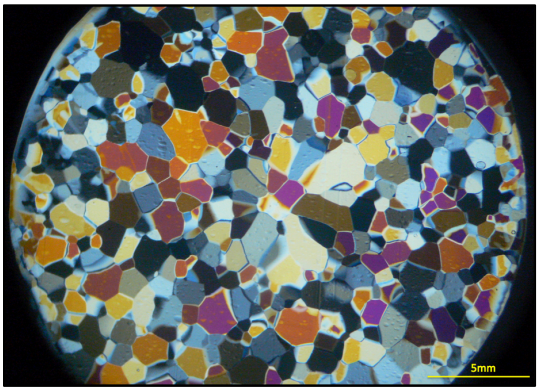

Fig. 1: Polycrystalline ice specimen as viewed through crossed polarized filters at 10x magnification.

From this originally cylindrical specimen of polycrystalline ice, we cut out ice lenses of a desired thickness for testing with a precision band saw. After being cut to size, the ice lens is placed between two layers of naturally collected (more than one year old) equi-temperature snow with a mean grain size between 2.5 and 3 mm. The setup is all contained in a 50 mm tall x 20 mm diameter polycarbonate tube with press-fit copper caps of 4 mm thickness, designed to seal the sample from any exterior influences other than the imposed temperature gradient (Fig. 2). Once the ice/snow sample has been created and all components loaded into the polycarbonate tube, the tube itself is placed in an insulated sleeve of polystyrene foam and placed into the temperature gradient controlling apparatus. The temperature gradient is controlled by two peltier cooling devices that are in flush contact with the copper caps of the sample. Each peltier cooler has an accuracy of 0.1°C and together can accommodate a maximum temperature gradient of approximately -500°C/m. This temperature gradient controlling apparatus, as well as the μ-CT scanner, are both housed in a -7°C cold room in the Ice Research Laboratory at the Thayer School of Engineering.

3.1 Temporal analysis via μ-CT

In our μ-CT observations, we used a 40 kV, 250 mA X-ray beam and rotated the sample 180°

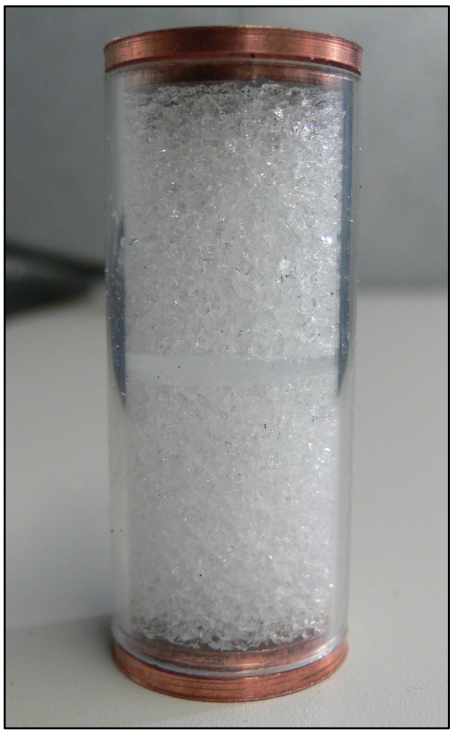

Fig. 2: Ice/snow sample with a 2 mm thick ice lens placed between natural snow of mean diameter 2.5-3 mm.

at 0.7° increments. This allowed for a 15 μm resolution to be obtained over a total scanning period of less than 20 minutes. For the portion of the experiment in which we were interested in quantifying the temporal effects of a constant temperature gradient held on our ice/snow sample, we chose a temperature gradient of -100°C/m. This equated to a temperature at the top and bottom of the sample of -12.3°C and -7.7°C, respectively. Our convention for the direction of the temperature gradient and magnitude was intended to mimic a relatively warm ground surface that had been covered by a thin snowpack, as is common in many mountainous winter environments. After an initial μ-CT scan was performed to capture the zero-hour initial conditions, the ice/snow sample was successively scanned in 6 h intervals for a 48 h period. Although the sample had to be removed from the temperature gradient apparatus for each scanning period, this was typically no longer than 25 min in duration and did not appear to have any noticeable effect on our observations. Thus far, we have analyzed ice lens thicknesses of 2, 4, and 8 mm. Following each scan, we then performed a detailed analysis of the 1.5 mm above and below the ice lens, as well as of the ice lens itself. Results from this analysis are given in Section 4.

3.2 *In situ micro-thermocouple measurements*

In order to capture the hypothesized temperature gradient that has been thought to exist at the ice/snow interface (see Section 1), we modified the polycarbonate tube by square milling the face of the tube into a flat surface and then drilling a series of 12 holes into the tube at specific locations. Each hole had a diameter of 360 μm, which allowed for the hand placement of our 80 μm, Teflon insulated, type-T micro-thermocouples. The placement of the holes was such that we would obtain two measurements in the bulk snow below the ice lens, four measurements within 1 mm below the ice lens at horizontally staggered 200 μm intervals, for a total of 12 temperature measurements after mirroring this configuration above the ice lens as well. To meet such stringent requirements of drilling accuracy, we used a high precision mill with 10 μm accuracy, located in the machine shop of the Thayer School of Engineering at Dartmouth. We were also able to later verify the placement of each micro-thermocouple with μ-CT images at the conclusion of each test (Fig. 3).

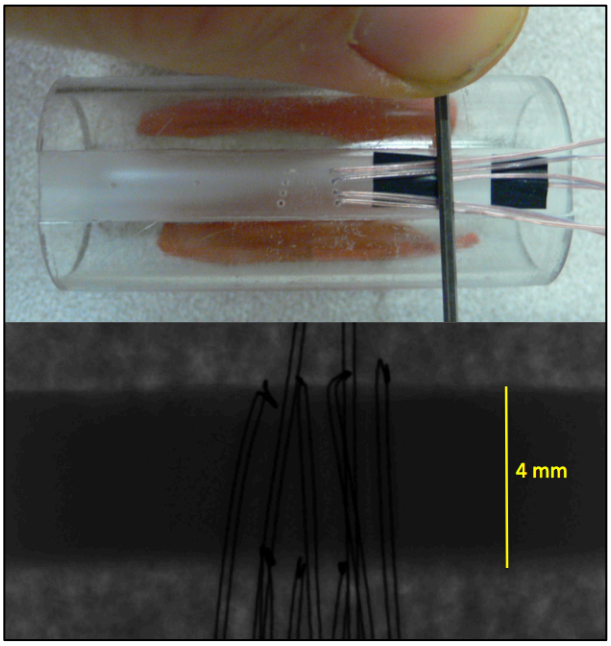

Fig. 3: Illustrations of micro-thermocouple placement within 1 mm of the ice lens surface before testing (top panel) and via post-test μ-CT verification (lower panel).

Once a sample was created and micro-thermocouples were appropriately placed, the sample was held under a constant temperature gradient for a 24 h period, assuring that steady state heat flow would be established within the sample. Temperatures were logged at 10 s intervals during this 24 h time period and the data was smoothed with a window-averaging filter before being analyzed. We have so-far only performed iterations of this testing procedure with a 4 mm thick ice lens and -100°C/m temperature gradient. To serve as a control, temperatures were also logged for a sample consisting of just snow and no ice lens, to assure all micro-thermocouples were functioning properly and calibrated appropriately.

4. OBSERVATIONS

Overall, our qualitative observations have been consistent with those made by Greene (2007), with regard to the kinetic growth of ice crystals on the lower surface of the ice lens while the top remained smooth. With regard to the development of micro-cavities above the ice lens that Greene observed, we were unable to make this observation directly, but this may be partly due to the rather large snow grains we used in our experiments, as compared to Greene (2007). Presented in this section, are the primarily qualitative observations made from our μ-CT and SEM analysis. Quantitative results from these observations are presented in Section 5.

4.1 *μ-CT observations*

Spatially, of the 20 mm circular diameter that was scanned for each test, we only performed analysis on the inner 14 mm diameter of the sample, in order to filter out any noise that may have been caused by edge effects or any inadvertent tilt of the sample while in the μ-CT. In the vertical direction, although the ice/snow sample itself stood 46 mm tall (less the copper caps) we only scanned the center 15 mm, positioned such that the ice lens would be in the center. This allowed us to use ice lenses of up to 8 mm in thickness while still leaving room to perform our detailed analysis on the 1.5 mm above and below the sample. A sample time-lapse sequence from one test run in which a 2 mm ice lens and a -100°C/m temperature gradient was used is shown in Fig. 4. In this figure, the qualitative observations consistent with Greene (2007) are quite clear. It should be noted, however, that although these time-lapse images are of the same sample, they are not necessarily from the same viewing angle and should not be misconstrued as representative of individual snow grain metamorphism.

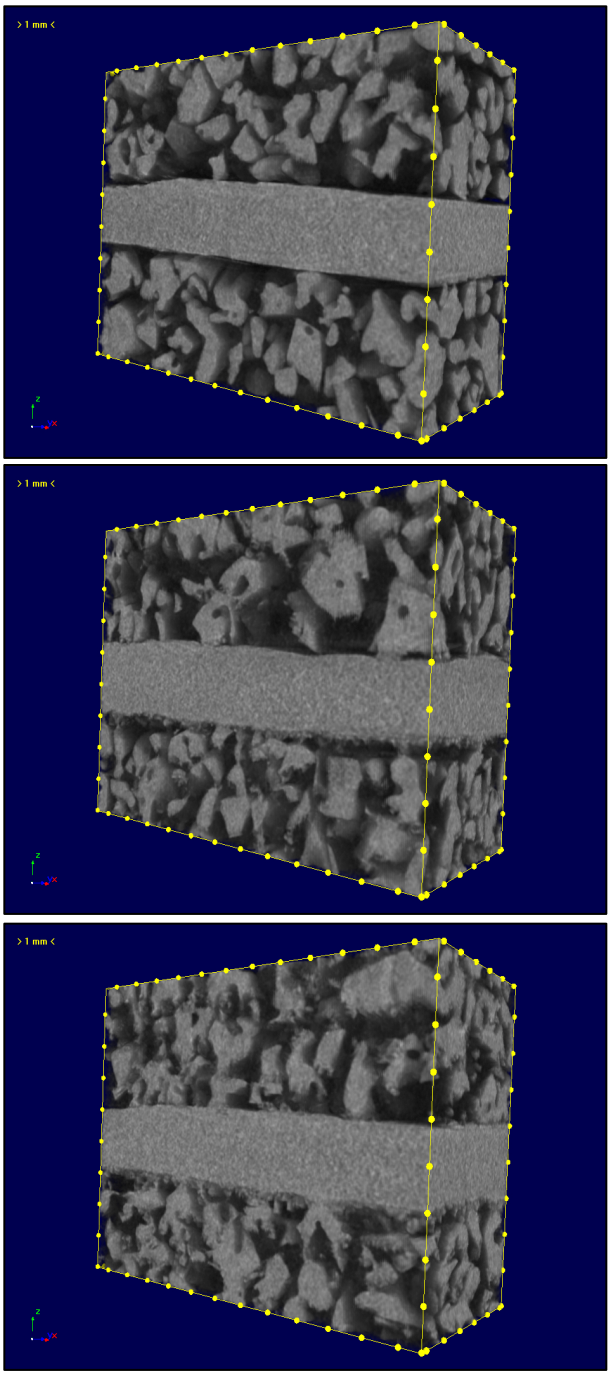

Fig. 4: Time lapse μ-CT reconstructions of a 2 mm thick ice lens evolving under a constant temperature gradient of -100°C/m over a 48 h period. Shown here are the 0, 24, and 48 h images.

4.2 SEM observations

Utilizing the SEM, we were able to broadly characterize the specific types of crystals that formed on the bottom surface of the ice lens, as well as verify that there was indeed no growth occurring on the top surface of the ice lens (Fig. 5).

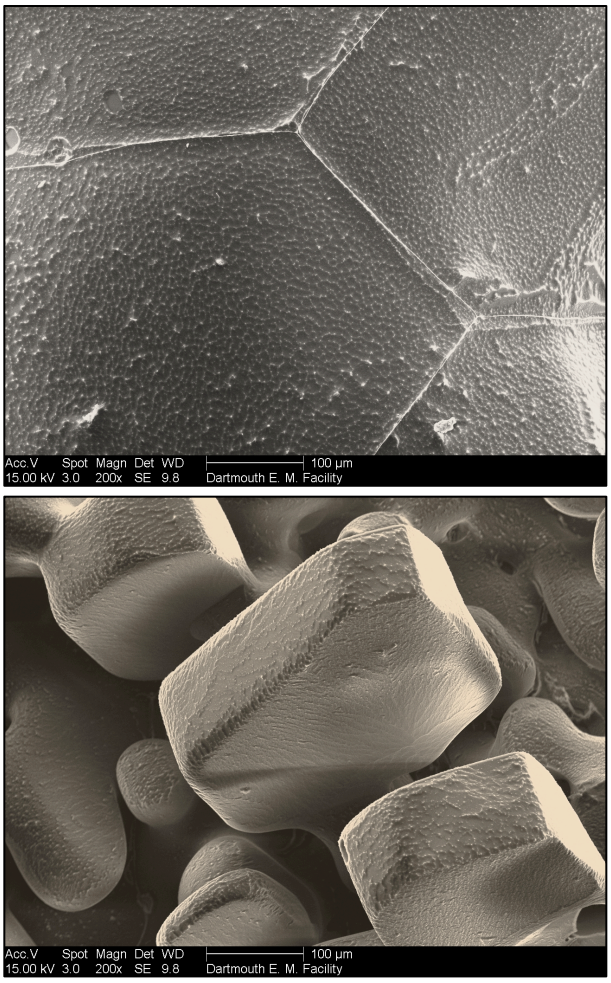

Fig. 5: SEM images of the top of an 8 mm thick ice lens (upper panel) compared to the bottom of the same ice lens (lower panel), after 48 hours of an imposed -100°C/m temperature gradient.

Looking across all the SEM images taken, it did not appear that the newly-formed ice crystals had any apparent preference in crystallographic orientation or plane of deposition (prismatic vs. basal planes). They were all sharply cornered and with large variation in their size and shape. What did seem to be occurring preferentially was the location of the deposition on the ice lens itself. Similar to the observations made in Greene (2007), we observed preferential kinetic ice crystal growth that occurred primarily on the raised or “ridged” sections of the ice lens. This striated or “ridged” pattern was left by the band saw when the ice lens was originally cut and seems to have acted as the preferred point for ice crystal nucleation, which would somewhat be expected due to the higher

surface energy and consequently lower contact angle needed for heterogeneous nucleation to occur (Pruppacher and Klett 1997).

5. ANALYSIS

While this study is still ongoing, it has already produced some interesting results. In addition to obtaining *in-situ* measurements of a super-temperature gradient near the ice lens, we have also seen a stark contrast between the increase of the specific surface area above and below the ice lens, which appears to have a correlation to the thickness of the ice lens itself. These and other tentative results are outlined below.

5.1 Micro-thermocouple results

Presented here are our findings from two independent temperature gradient experiments as described in Section 3.2. In the first experiment, we used a 4 mm thick ice lens and held a constant temperature gradient of -100°C/m while logging the temperature every 10 s for 24 h. After noise-filtering the results via a window-averaging filter, we took the mean temperature and plotted it as a function of height (Fig. 6). Also plotted on this figure is the linear temperature gradient for reference, which was used to calibrate the micro-thermocouple array. The red vertical hash bars in the figure mark the error associated with the measurements, which account for the standard deviation of the sample mean as well as the inherent measurement error associated with the micro-thermocouples and datalogger. The horizontal black lines show the approximate boundaries of the ice lens.

Our results show local temperature gradients within 1 mm of the ice lens surface to be approximately -300°C/m above and -600°C/m below. These observations are in direct support of our working hypothesis which assumes a super-temperature gradient must exist at the snow/ice interface, with an effective thermal conductivity different from that of ice or snow alone, as it also accounts for the latent heat term in Eq. 1. Also of interest in this figure is the nearly isothermal conditions that appear to exist within the first 7 mm of snow near the bottom of the ice/snow sample. We conjecture that this is evidence of the buoyancy force needed for convection to not be able to overcome the opposing force of viscosity of the water vapor in the pore space of the snow grains, as mentioned in Section 2, and also in support of our decision not to include an additional term for convection in Eq. 1. Had convection been a factor, we would have expected a more uniform temperature to have been observed in the region of the sample below the ice lens, as well as more uniformly mixed water vapor in the pore space of the snow grains.

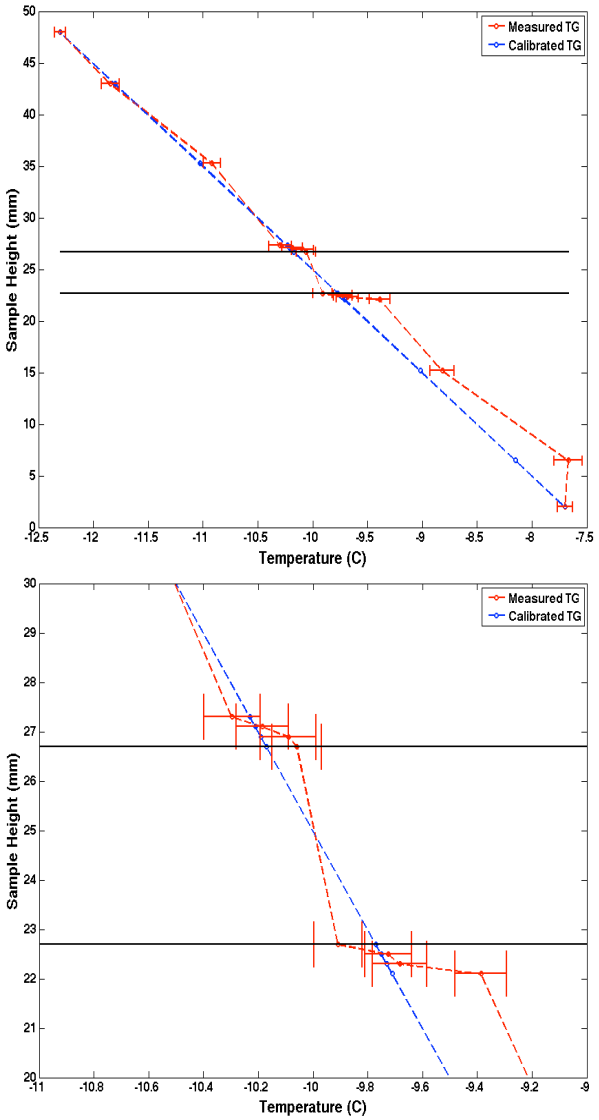

Fig. 6: Temperature gradient measurements after steady state heat flow was achieved with a 4 mm ice lens present in the sample.

5.2 μ-CT analysis

In our μ-CT analysis, we focused primarily on the ice lens itself and the 1.5 mm above and below the ice lens for three different experiments with ice lens thicknesses of 2, 4, and 8 mm, as described in Section 3.1. Of the numerous calculations that can be made from μ-CT reconstructions, we have chosen to focus for the time being only on the temporal evolution of the specific surface area (SSA) and the mean grain diameter, as these two

parameters have shown consistent trends across all experiments.

The SSA of the ice lens itself was found to increase in all three experiments, which would be expected after seeing the dramatic increase in the surface area in the SEM images, while the overall volume of the ice lens remained relatively constant. Because we know the top surface of the ice lens is only changing nominally in its surface area, this increase in the SSA can nearly be entirely attributed to the kinetic ice crystal growth occurring on the bottom of the ice lens. Therefore, the ice lens SSA can be thought of as a metric for how the newly formed ice crystals are growing over time, which appears to have a linear trend, as shown in the top panel of Fig. 7.

Our analysis of the SSA 1.5 mm directly above and below the ice lens was another approach to quantifying the effect that the kinetic ice crystal growth and temperature gradient was having on the overall SSA of these adjacent layers. In this analysis there appears to be a divergence between how the SSA changed over time as a function of both spatial location (above or below the ice lens) as well as with the changing ice lens thickness. As can be seen in the lower panel of Fig. 7, the SSA below the ice lens was generally increasing at a faster rate than above. This disparity is probably a combination of both differing rates of snow metamorphism and the fact that the new ice crystal growth was contributing much of the surface area to the SSA calculation in this region. How the thickness of the ice lens is related to these measurements is still under investigation, but it is hypothesized that because the thermal conductivity of solid polycrystalline ice is much greater than that of snow, it could be acting as a sort of heat reservoir for the local latent heat release occurring during deposition. If shown to be true in our future work, this would indicate that thicker ice lenses are more catalytic for ice deposition than thinner ice lenses, given that they are more efficient in conducting away the latent heat released, at least in a steady state sense.

Turning to grain size, the mean grain diameter 1.5 mm above and below the ice lens was calculated as part of the degree of anisotropy calculation for the layer, which is not shown here but requires a 3-D perspective on the region of interest meaning that the mean grain diameter is also a 3-D characterized quantity. Having started with old, isothermal, naturally collected snow for our initial conditions, it is not too surprising that the mean grain diameter was observed to decrease overall

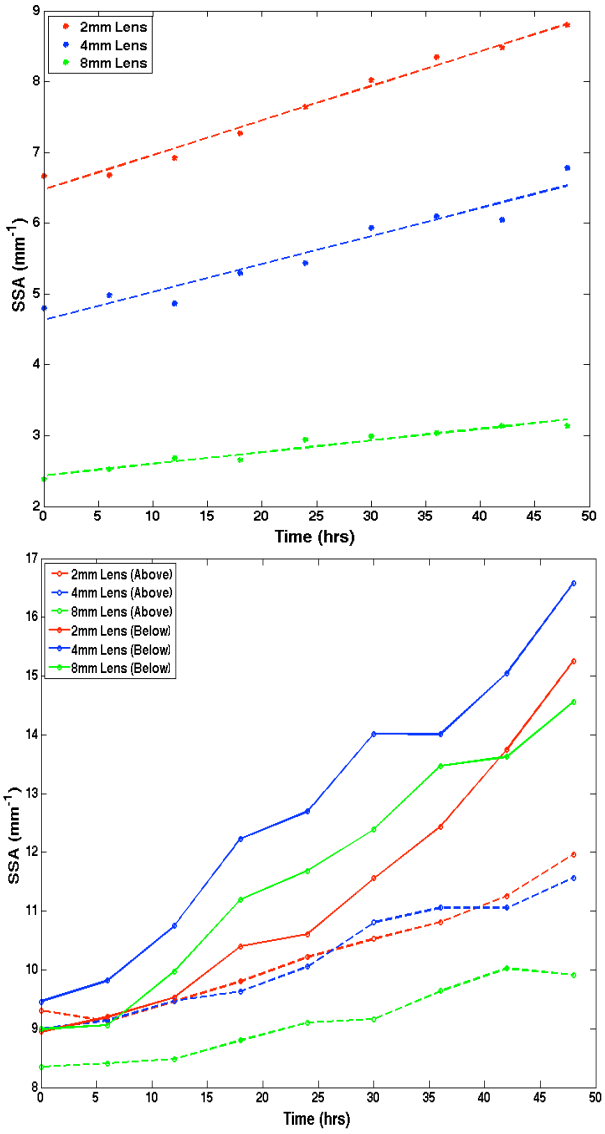

Fig. 7: SSA calculations for each ice lens (upper panel) and 1.5 mm above and below each ice lens (lower panel). Dashed lines in the upper panel show the best fit of data via a linear regression.

when placed under a large temperature gradient. Of particular interest, however, was the rate at which the mean grain diameter decreased below the ice lens as opposed to above it (Fig. 8). Whether or not this apparent effect can be directly correlated to the local temperature gradient below the ice lens being a factor of two larger than above the ice lens, remains unclear. It is most likely a combination of the larger local temperature gradient combined with the presence of the newly formed ice crystals (small in size and large in number) being included in the calculation for this region. In our future work, we intend to segregate

these two very independent populations and for the time being acknowledge that we do not have a firm explanation for the trends observed in Fig. 8.

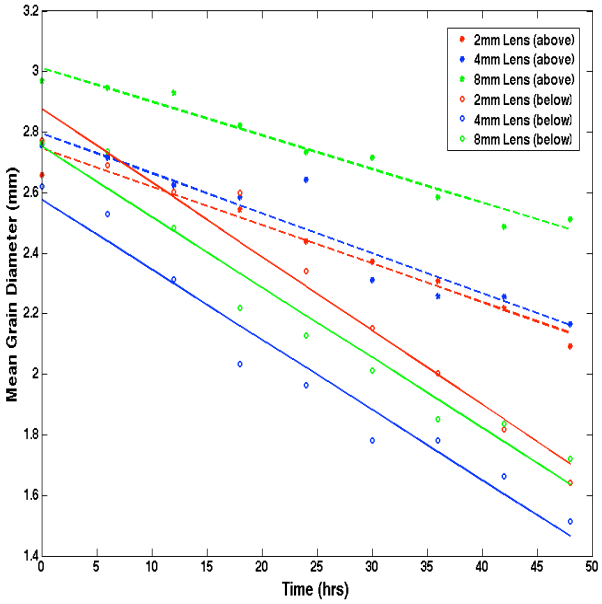

Fig. 8: Mean grain diameter as a function of time 1.5 mm above and below the ice lens. Straight lines show best fit of data via linear regression.

6. CONCLUSIONS

In this study, we have demonstrated a laboratory technique for studying the effects that an artificial ice lens can have on the thermophysical properties and resultant metamorphic state of the surrounding layers of snow. Our results show that there is a local temperature gradient that exists near the ice lens surface at the snow/ice interface that can be as much as a factor of six times larger than the imposed bulk temperature gradient below the ice lens and a factor of three times larger above. This is thought to be a significant finding as there is a large number of avalanches that have been reported to occur either on or near these ice/snow interfaces in natural snowpacks. We have also been able to further solidify earlier qualitative observations made by Greene (2007) via μ-CT and SEM analysis that show one-sided kinetic ice crystal growth as a result of a uni-directional temperature gradient. Combined, these observations and results build a very effective phenomenological model for enhanced instability in a snowpack due to the presence of an impermeable ice lens. In our future work, we intend to include the effects of additional temperature gradients and variations in ice lens thickness, which we hope will ultimately be able to serve as a new field metric for the correlation between observed temperature gradients and kinetic snow metamorphism near an ice lens.

ACKNOWLEDGEMENTS

This work was supported by the Theo Meiners Research Grant awarded on behalf of the American Avalanche Association, the National Science Foundation grant number PLR 1141411, and the U.S. Army Corps of Engineers, Cold Regions Research and Engineering Laboratory. The authors acknowledge the use of the Ice Research Laboratory (Director E.M. Schulson) at the Thayer School of Engineering.

REFERENCES

Armstrong, R.L., 1985: Metamorphism in a subfreezing, seasonal snow cover: The role of thermal and vapor pressure conditions, Ph.D. Dissertation, University of Colorado, 175 pp.

Adams, E.E., and R.L. Brown, 1990: A mixture theory for evaluation heat and mass transport processes in nonhomogeneous snow. *Continuum Mechanics and Thermodynamics,* **2**, 31-63.

Colbeck, S.C., 1991: The layered character of snow covers. *Reviews of Geophysics*, **29**, 81-96.

Colbeck, S.C., and J.B. Jamieson, 2001: The formation of faceted layers above crusts. *Cold Regions Science and Technology*, **33**, 247-252.

Cole, D.M., 1979: Preparation of polycrystalline ice specimens for laboratory experiments. *Cold Regions Science and Technology,* **1**, 153-159.

Courville, Z.R., 2007: Gas diffusivity and air permeability of the firn from cold polar sites, Ph.D. Dissertation, Thayer School of Engineering at Dartmouth College, 197 pp.

Gibson, L.J., and M.F. Ashby, 1997: *Cellular Solids: Structure and Properties,* Cambridge University Press, 532 pp.

Greene, E.M., 2007: The thermophysical and microstructural effects of an artificial ice layer in natural snow under kinetic growth metamorphism. Ph.D. Dissertation, Colorado State University, 147 pp.

Pruppacher, H.R. and J.D. Klett, 1978: *Microphysics of Clouds and Precipitation.* D. Reidel, 714 pp.